

## IN-SILICO EVALUATION OF HERBAL COMPOUNDS TARGETING INHA OF MYCOBACTERIUM TUBERCULOSIS BY MOLECULAR DOCKING

Ronak Patadiya<sup>1</sup>, Sangita Shukla<sup>1</sup>, Nikunj Patadiya<sup>2\*</sup>

<sup>1</sup>Department of Pharmacognosy, Indubhai Patel College of Pharmacy and Research Center, Dharmaj, Gujarat, India.

<sup>2</sup>Research Scholar, Gujarat Technological University, Ahmedabad, Gujarat, India.



\*Corresponding Author: Nikunj Patadiya

Research Scholar, Gujarat Technological University, Ahmedabad, Gujarat, India.

DOI: <https://doi.org/10.5281/zenodo.18958287>

**How to cite this Article:** Ronak Patadiya<sup>1</sup>, Sangita Shukla<sup>1</sup>, Nikunj Patadiya<sup>2\*</sup>. (2026). IN-Silico Evaluation of Herbal Compounds Targeting Inha of Mycobacterium Tuberculosis By Molecular Docking. European Journal of Pharmaceutical and Medical Research, 13(3), 566–575.

This work is licensed under Creative Commons Attribution 4.0 International license.



Article Received on 15/02/2026

Article Revised on 05/03/2026

Article Published on 10/03/2026

### ABSTRACT

The present study aimed to evaluate the inhibitory potential of selected plant-derived compounds against the target protein (PDB ID: 4TZK) through molecular docking analysis. The three-dimensional structure of the protein was retrieved from the RCSB Protein Data Bank and docking simulations were performed using PyRx. A total of ten phytochemicals—Bilobetine, Tetrandrine, Lobenine, Nolatrexed, Sophoraflavanone G, Isoquirigenine, Luteolin, Aloin, Cinchonine, and Licochalcone A—were evaluated, with Isoniazid used as the reference drug. The docking results revealed that all selected compounds exhibited stronger binding affinities than Isoniazid (−5.2 kcal/mol). Among them, Bilobetine demonstrated the highest binding affinity (−10.4 kcal/mol), followed by Tetrandrine and Lobenine (−8.9 kcal/mol). Interaction analysis indicated the involvement of key active-site residues, including TYR-158, PHE-149, MET-199, and ILE-194, through hydrogen bonding,  $\pi$ - $\pi$  stacking, and hydrophobic interactions. Structure–activity relationship analysis suggested that aromatic ring systems, hydroxyl substitutions, and hydrophobic moieties significantly contribute to enhanced binding stability. Overall, the findings indicate that these phytochemicals possess promising inhibitory potential and warrant further experimental validation for therapeutic development.

**KEYWORDS:** Tuberculosis, Anti-tubercular agent, InhA inhibitors, Plant molecules.

### INTRODUCTION

Tuberculosis (TB) is an infectious disease caused by the *Mycobacterium tuberculosis* (Mtb) and stands as a significant contributor to global morbidity and mortality.<sup>[1]</sup> The disease is spread through the inhalation of aerosolized droplets expelled by TB-infected individuals during coughing, sneezing, or spitting. These droplets can remain suspended in the air and may be inhaled by others. Although TB is both preventable and curable with proper treatment, it remains a serious global health problem. It is estimated that nearly one-quarter of the world's population has been infected with TB bacteria, although not all infected individuals develop active disease.<sup>[2]</sup> People with weakened immune systems, such as those suffering from HIV infection, diabetes, malnutrition, or other chronic illnesses, are at a higher risk of developing active TB compared to healthy individuals.<sup>[3]</sup> TB can be classified in several ways

depending on its clinical presentation and infection status. Clinically, TB is divided into pulmonary TB and extrapulmonary TB. Pulmonary TB affects the lungs and is the most common and infectious form of the disease.<sup>[4]</sup> Extrapulmonary TB occurs when the infection spreads outside the lungs to organs such as lymph nodes, bones, kidneys, meninges, or the pleura. This spread usually happens through the bloodstream (hematogenous dissemination) or by direct extension from nearby infected tissues.<sup>[4,5]</sup> Based on infection status, TB is categorized as latent TB infection (LTBI) or active TB disease.<sup>[6]</sup> Latent TB refers to a condition in which a person is infected with *Mycobacterium tuberculosis* but does not show symptoms and cannot spread the disease to others.<sup>[6]</sup> However, latent TB can become active if the immune system becomes weak.<sup>[6]</sup> Active TB disease occurs when the bacteria multiply and cause clinical symptoms such as persistent cough, fever, night sweats,

weight loss, and fatigue.<sup>[7]</sup> When active TB affects the lungs or throat, it can spread to other people, whereas TB affecting organs like the kidney or spine is usually not infectious.<sup>[6,7]</sup>

The history of tuberculosis dates back thousands of years. Evidence of TB has been found in ancient skeletal remains and Egyptian mummies, showing that the disease has affected humans since early civilizations.<sup>[8]</sup> In ancient Greece, TB was known as “phthisis,” a term used to describe wasting diseases.<sup>[9]</sup> Hippocrates provided one of the earliest clinical descriptions of TB and noted that it commonly affected young adults between eighteen and thirty-five years of age. These historical records demonstrate that TB has long been recognized as a serious and often fatal disease.<sup>[10-12]</sup>

Worldwide, TB is the 13th leading cause of death and the second leading infectious killer after COVID-19 (above HIV/AIDS). It is estimated that up to one-third of population is infected with *Mycobacterium*. In 2020, an estimated 10 million people fell ill with tuberculosis (TB) worldwide including 5.6 million men, 3.3 million women and 1.1 million children which shows that TB is present in all age groups. Child and adolescent TB is often overlooked by health providers and can be difficult to diagnose and treat. In 2020, the 30 high TB burden countries accounted for 86% of new TB cases. Eight countries account for two thirds of the total, with India leading the count, followed by China, Indonesia, the Philippines, Pakistan, Nigeria, Bangladesh and South Africa. Multidrug-resistant TB (MDR-TB) remains a public health crisis and a health security threat. Only about one in three people with drug resistant TB accessed treatment in 2020. Globally, TB incidence is falling at about 2% per year and between 2015 and 2020 the cumulative reduction was 11%. This was over halfway to the end TB strategy milestone of 20% reduction between 2015 and 2020. TB remains a leading cause of global morbidity and mortality. According to the WHO Global TB Report 2023, about 10.6 million people developed TB and 1.3 million people died in 2022.<sup>[13]</sup> TB is more common in low- and middle-income countries, with high burdens reported in Africa and South-East Asia.<sup>[13-14]</sup> Major risk factors include HIV co-infection, diabetes, malnutrition, smoking, and poverty.<sup>[15-17]</sup>

The pathophysiology of TB begins when a person inhales airborne droplet nuclei containing *Mycobacterium tuberculosis*.<sup>[18]</sup> These tiny particles travel deep into the lungs and reach the alveoli. There, alveolar macrophages ingest the bacteria in an attempt to destroy them. However, *Mycobacterium tuberculosis* has developed survival mechanisms that allow it to resist destruction inside macrophages. It prevents the fusion of phagosomes with lysosomes and neutralizes acidic conditions within the cell. As a result, the bacteria can survive and multiply within immune cells. This leads to activation of inflammatory pathways and recruitment of additional immune cells to the infection site.<sup>[19]</sup> The

immune system forms a granuloma, which is a structured collection of immune cells that attempts to contain the infection. In many individuals, the bacteria remain dormant inside granulomas, resulting in latent TB.<sup>[20]</sup> If the immune system weakens, the granuloma may break down, leading to active TB disease. In active TB, tissue destruction and caseous necrosis can occur, forming cavities in the lungs and allowing bacteria to spread through coughing.<sup>[18-20]</sup> The bacteria may also spread through blood and lymphatic vessels to other organs, causing extrapulmonary TB.<sup>[18-20]</sup> Therefore, the outcome of TB infection depends largely on the balance between bacterial virulence and host immune response.<sup>[20,21]</sup>

The treatment of TB improved significantly after the discovery of streptomycin in 1943, followed by the introduction of isoniazid and rifampicin.<sup>[22-23]</sup> These drugs formed the foundation of modern anti-TB therapy. However, the development of drug resistance has become a serious obstacle in TB control.<sup>[14]</sup> Resistance to first-line drugs such as isoniazid (INH), rifampicin, ethambutol, and pyrazinamide complicates treatment and increases mortality.<sup>[14-24]</sup> INH is a prodrug that requires activation by the KatG enzyme to inhibit enoyl-acyl carrier protein reductase (InhA), a crucial enzyme of the fatty acid synthase-II (FAS-II) pathway responsible for mycolic acid biosynthesis.<sup>[25]</sup> Mutations in KatG impair INH activation, leading to resistance.<sup>[25]</sup> To overcome this, research has focused on direct InhA inhibitors that bypass KatG and selectively block the enzyme. Several scaffolds, including triclosan, diphenyl ethers, arylamides, pyrrolidines, and pyrimidines, have shown promise as InhA inhibitors.<sup>[26-27]</sup>

Chalcones are chemical compounds synthesized through aldol condensation and are known for their wide range of biological activities, including antibacterial, anti-inflammatory, antifungal, and anticancer properties. Several chalcone derivatives have demonstrated significant anti-tubercular activity.<sup>[28]</sup> Pyrimidines represent another important class of antimicrobials, and isoniazid-pyrimidine conjugates have demonstrated strong antimycobacterial efficacy.<sup>[29]</sup> Pyrroles and their derivatives, including LL3858 (Sudoterb), have shown significant antitubercular activity in preclinical studies.<sup>[30]</sup> Recent strategies propose combining chalcone, pyrimidine, and pyrrole frameworks to design novel InhA inhibitors with enhanced potency.<sup>[28-30]</sup> These advances highlight InhA inhibitors as a promising direction in overcoming drug-resistant TB.<sup>[31-42]</sup>

## MATERIALS AND METHODS

The three-dimensional crystal structure of the target protein (PDB ID: 4TZK)<sup>[43]</sup> was retrieved from the RCSB Protein Data Bank. The protein structure was prepared prior to docking by removing co-crystallized ligands and water molecules, followed by the addition of polar hydrogen atoms and appropriate charge assignment. The prepared protein structure was saved in PDB format for subsequent analysis.

The chemical structures of the selected phytocompounds—Bilobetine, Tetrandrine, Lobenine, Nolatrexed, Sophoraflavanone G, Isoquirigenine, Luteolin, Aloin, Cinchonine, and Licochalcone A—were obtained from the ChemSpider database. The standard anti-tubercular drug Isoniazid was used as the reference compound for comparative analysis. All ligand structures were downloaded in suitable file formats and subjected to energy minimization prior to docking. The minimized ligands were then converted into the required format compatible with the docking software.<sup>[44-46]</sup>

Molecular docking simulations were performed using PyRx, which incorporates the AutoDock Vina algorithm for virtual screening and binding affinity prediction. Docking was carried out under default parameters, and binding energies were recorded in kcal/mol. The grid box was defined to encompass the active site region of the target protein to ensure accurate interaction analysis.<sup>[47-49]</sup>

Post-docking interaction analysis was conducted using Discovery Studio Visualizer to evaluate hydrogen bonding, hydrophobic interactions, and other non-covalent interactions between the protein and ligands through both two-dimensional and three-dimensional visualization. Docking scores and interaction data were compiled and comparatively analyzed using Microsoft Excel to identify the most promising compounds based on binding affinity relative to the reference drug.<sup>[50-55]</sup>

## RESULTS AND DISCUSSION

### Molecular docking

The molecular docking analysis of selected phytocompounds against the target protein (PDB ID: 4TZK) revealed significant variations in binding affinity and interaction patterns compared with the reference drug, Isoniazid (Table:1). The reference compound exhibited a binding affinity of  $-5.2$  kcal/mol and formed a conventional hydrogen bond with ILE-194, along with  $\pi$ - $\pi$  stacking interaction with PHE-149 and hydrophobic interaction with MET-199. These interactions served as a benchmark for evaluating the binding efficiency of the tested plant-derived compounds.

Among the screened phytochemicals, Bilobetine demonstrated the strongest binding affinity ( $-10.4$  kcal/mol), indicating a markedly higher binding potential than the reference drug. Bilobetine formed multiple hydrogen bonds with LYS-165, MET-147, GLY-96, and MET-98, along with  $\pi$ - $\pi$  stacking interaction with PHE-148 and hydrophobic interactions involving MET-199, ALA-198, and LEU-207, suggesting stable accommodation within the active site. Tetrandrine and Lobenine also exhibited strong binding affinities ( $-8.9$  kcal/mol each). Tetrandrine showed hydrophobic interactions with ALA-198, ILE-16, MET-199, and TYR-158, whereas Lobenine formed hydrogen bonds with SER-94, ILE-21, ALA-22, and TYR-158, along with  $\pi$ - $\pi$  stacking interaction with PHE-149 and hydrophobic contact with MET-147.

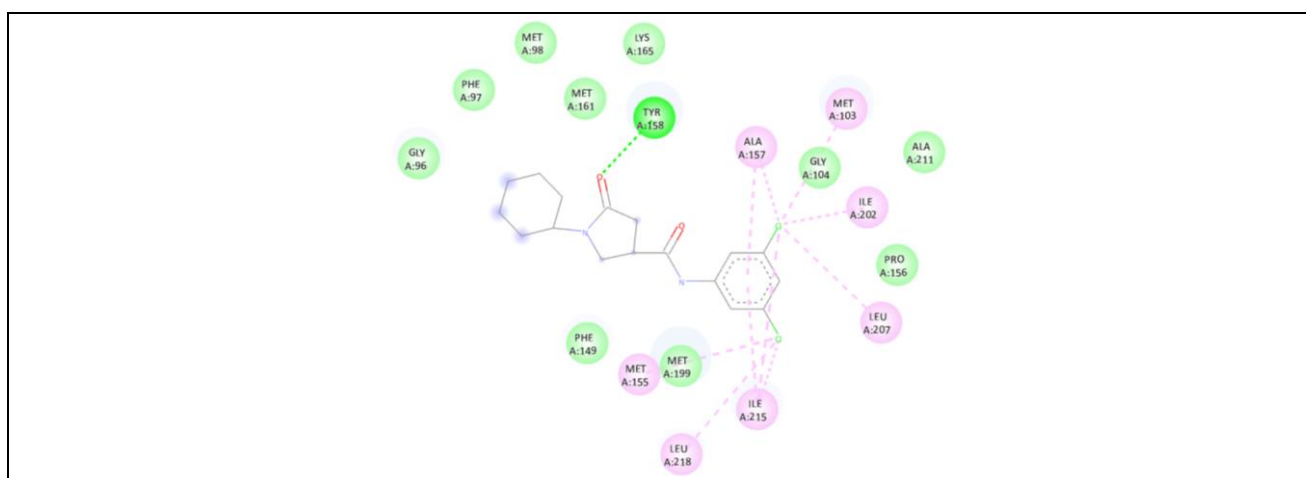
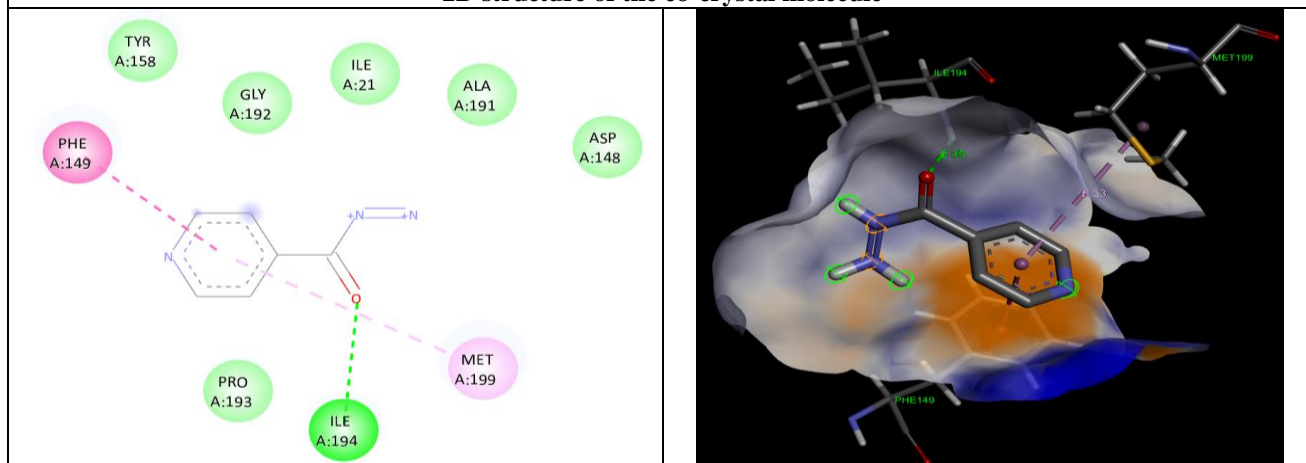
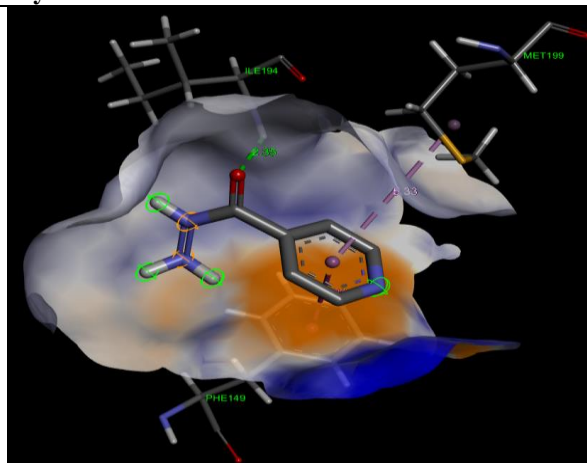
Nolatrexed demonstrated a binding affinity of  $-8.8$  kcal/mol, forming hydrogen bonds with TYR-158 and LYS-165 and hydrophobic interactions with ALA-191 and ILE-21, alongside  $\pi$ - $\pi$  stacking with PHE-149. Sophoraflavanone G ( $-8.6$  kcal/mol) interacted through hydrogen bonds with MET-199 and ILE-194 and showed additional hydrophobic contacts with MET-161, ILE-215, and PHE-149. Isoquirigenine and Luteolin both exhibited binding affinities of  $-8.2$  kcal/mol; Isoquirigenine formed a hydrogen bond with MET-155 and hydrophobic interaction with ALA-157, while Luteolin established a hydrogen bond with PRO-156 and displayed  $\pi$ - $\pi$  stacking with PHE-149 and hydrophobic interactions involving ILE-215, ALA-157, and MET-199.

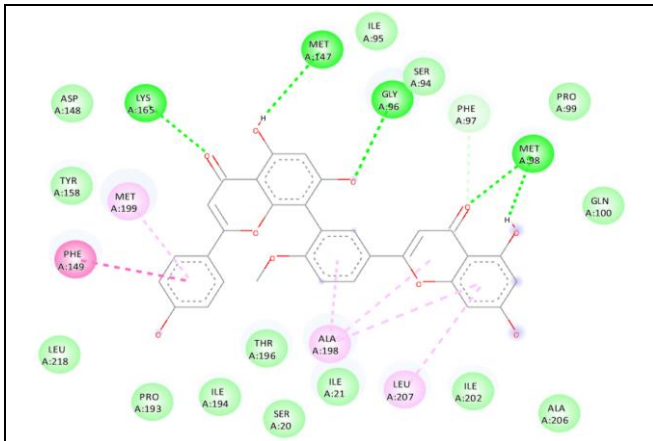
Aloin and Cinchonine each showed binding affinities of  $-8.1$  kcal/mol. Aloin formed hydrogen bonds with ILE-194, SER-20, and SER-94 and hydrophobic interactions with ALA-198 and ILE-21. Cinchonine demonstrated hydrophobic interactions with MET-199, PHE-149, PRO-193, and LEU-218. Licochalcone A exhibited a binding affinity of  $-7.8$  kcal/mol and showed hydrophobic interactions with MET-161, ALA-191, ILE-215, and PHE-142.

Overall, all selected phytocompounds demonstrated stronger binding affinities than the reference drug Isoniazid. Notably, Bilobetine showed the highest binding affinity and formed multiple stabilizing interactions within the active site, suggesting its potential as a promising inhibitor of the target protein. The presence of key interacting residues such as PHE-149, MET-199, TYR-158, and ILE-194 across several docked complexes indicates their critical role in ligand stabilization. These findings suggest that the studied plant-derived compounds may serve as potential lead molecules for further in vitro and in vivo validation studies. 2D and 3D dock poses of co-crystal ligand, Isoniazid and studied molecules show in fig.1

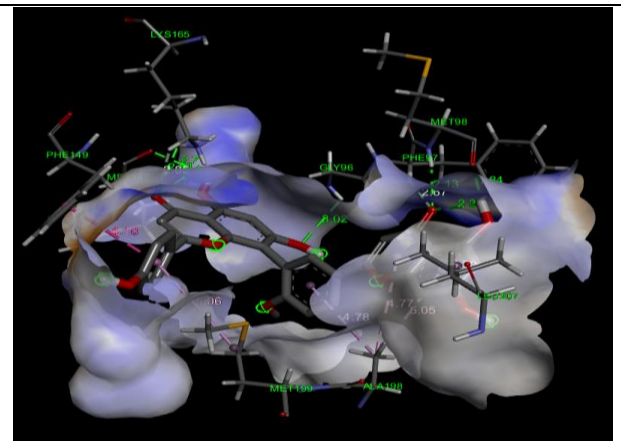
**Table 1: Binding affinity and type of interactions of phytoconstituents with InhA enzyme.**

| Compound name    | Binding affinity (kcal/mol) (dock score) | H-bond                           | $\pi$ - $\pi$ stacking | $\pi$ - alkyl   | Alkyl            | $\pi$ - sigma |
|------------------|--|----------------------------------|------------------------|---|------------------|---------------|
| Co-crystal       |  | TYR-158                          |                        | ALA-157, MET-103, ILE-202, LEU-207, ILE-215, LEU-218, MET-155 |                  |               |
| Isoniazid        | -5.2                                     | ILE-194                          | PHE-149                | MET-199   |                  |               |
| Bilobetine       | -10.4                                    | LYS-165, MET-147, GLY-96, MET-98 | PHE-148                | MET-199, ALA-198, LEU-207                                     |                  |               |
| Tetrandrine      | -8.9                                     |                                  |                        | ALA-198, ILE-16   | MET-199, TYR-158 |               |
| Lobenine         | -8.9                                     | SER-94, ILE-21, ALA-22, TYR-158  | PHE-149                |   | MET-147          |               |
| Nolatrexed       | -8.8                                     | TYR-158, LYS-165                 | PHE-149                |   | ALA-191, ILE-21  |               |
| Sophaflavanone G | -8.6                                     | MET-199, ILE-194                 |                        | MET-161   | ILE-215          | PHE-149       |
| Isoquirigenine   | -8.2                                     | MET-155                          |                        | ALA-157   |                  |               |
| Luteolin         | -8.2                                     | PRO-156                          | PHE-149                | ILE-215, ALA-157, MET-199                                     |                  |               |
| Aloin            | -8.1                                     | ILE-194, SER-20, SER-94          |                        | ALA-198, ILE-21   |                  |               |
| Cinchonine       | -8.1                                     |                                  |                        | MET-199, PHE-149, PRO-193                                     | LEU-218          |               |
| Licochalcone A   | -7.8                                     |                                  |                        | MET-161, ALA-191  | ILE-215          | PHE-142       |

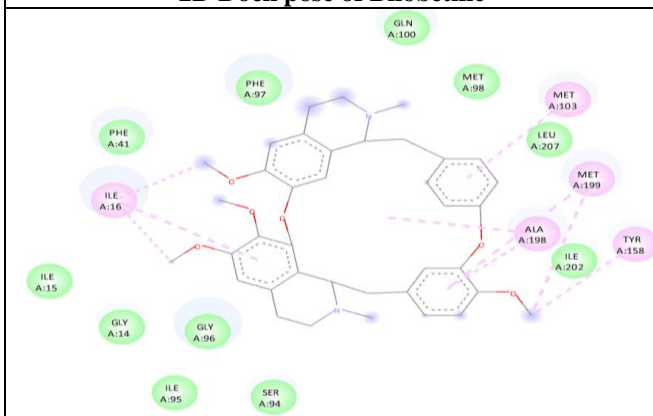
**2D structure of the co-crystal molecule****2D dockpose of Isoniazide****3D dockpose of Isoniazide**



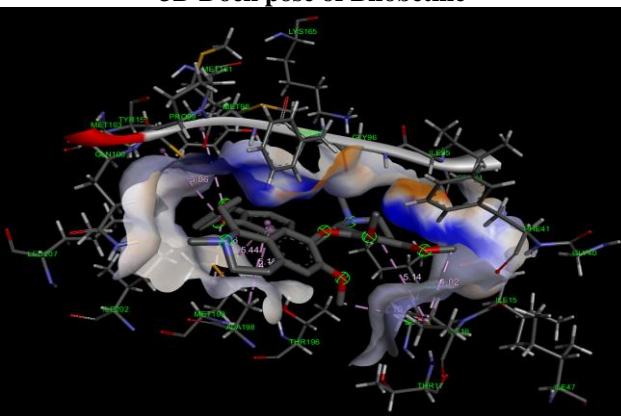
2D Dock pose of Bilobetine



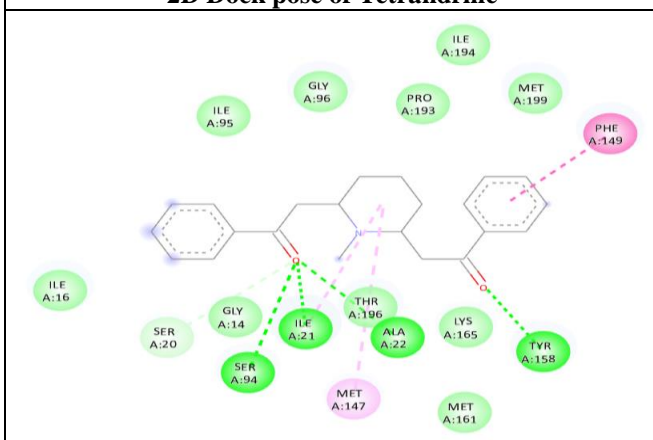
3D Dock pose of Bilobetine



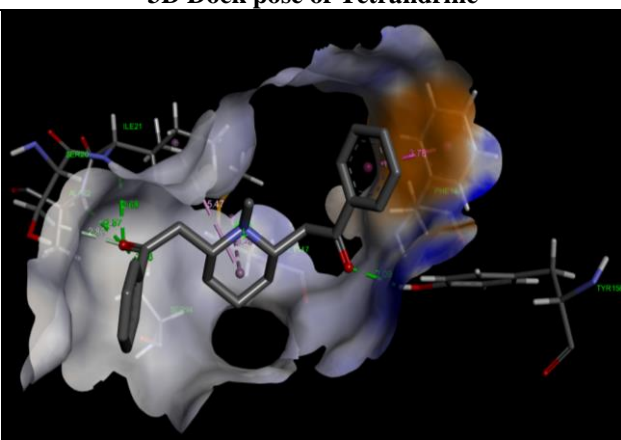
2D Dock pose of Tetrandrine



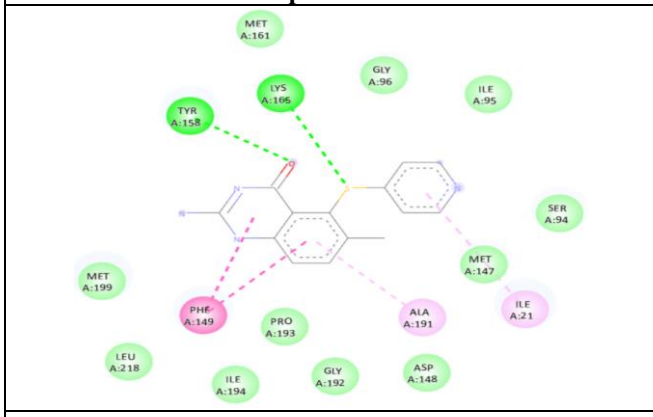
3D Dock pose of Tetrandrine



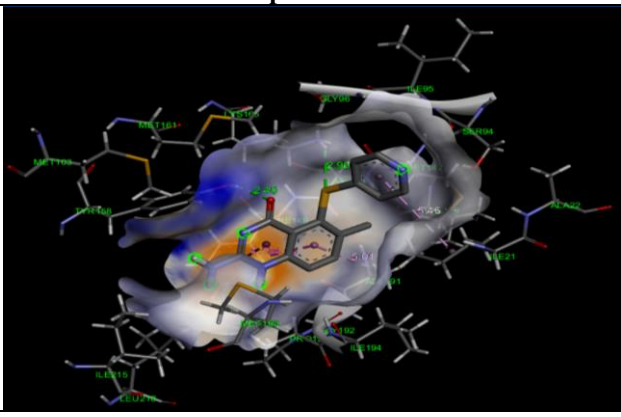
2D Dock pose of Lobenine



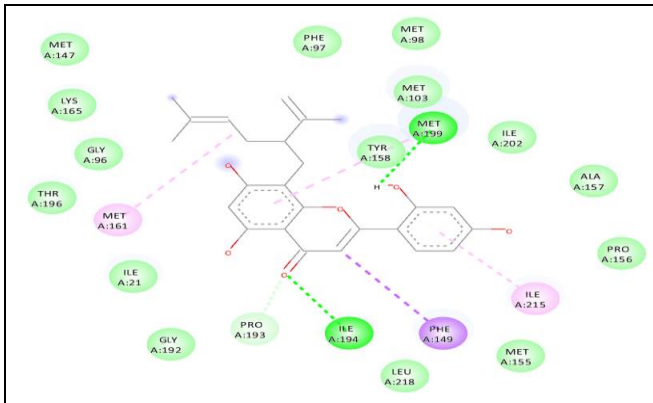
3D Dock pose of Lobenine



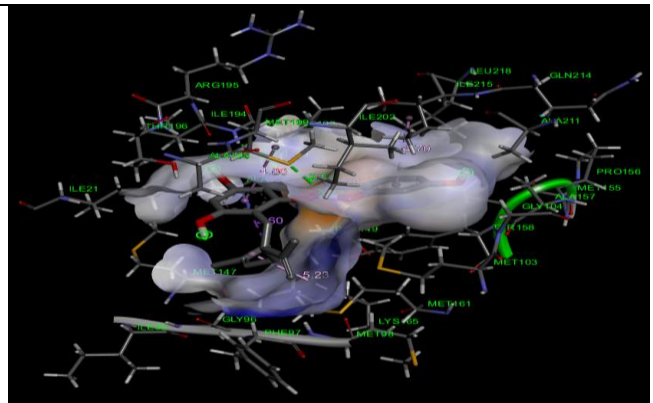
2D Dock pose of Nolatrexed



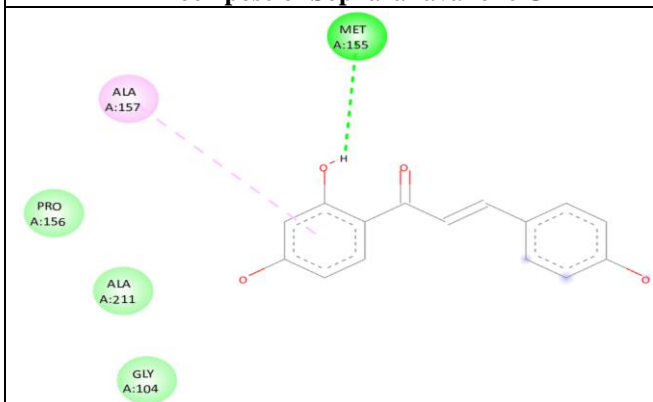
3D Dock pose of Nolatrexed



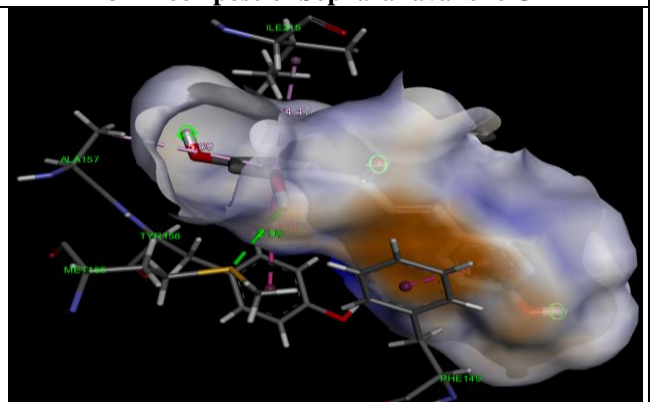
2D Dock pose of Sophoraflavanone G



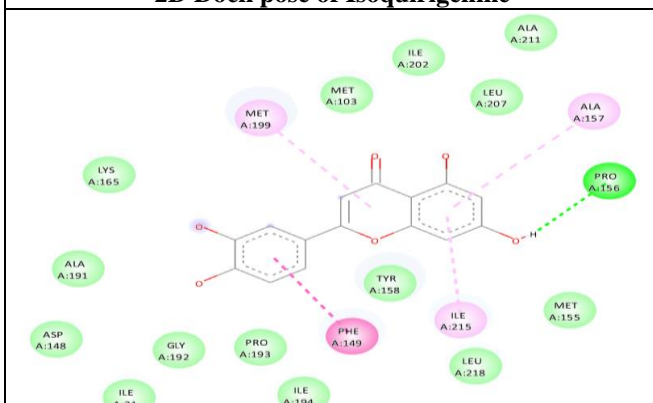
3D Dock pose of Sophoraflavanone G



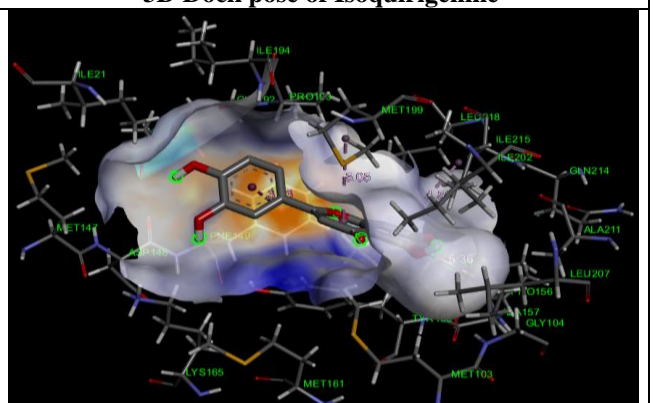
2D Dock pose of Isoquiritigenine



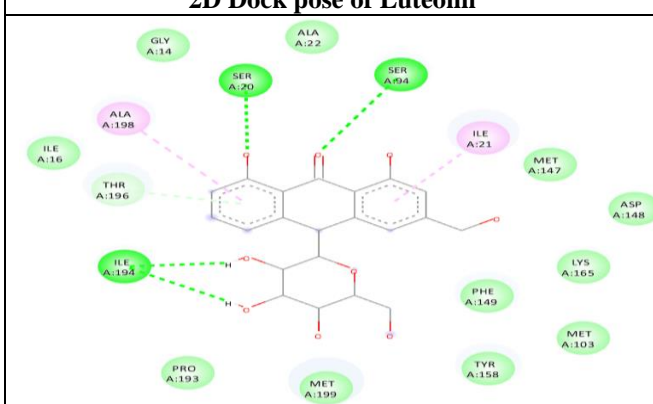
3D Dock pose of Isoquiritigenine



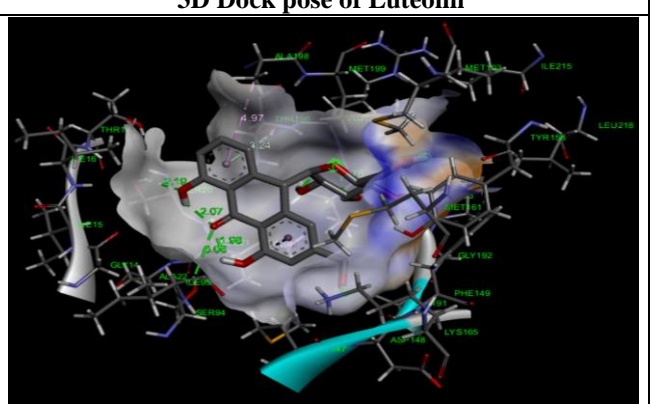
2D Dock pose of Luteolin



3D Dock pose of Luteolin



2D Dock pose of Aloin



3D Dock pose of Aloin

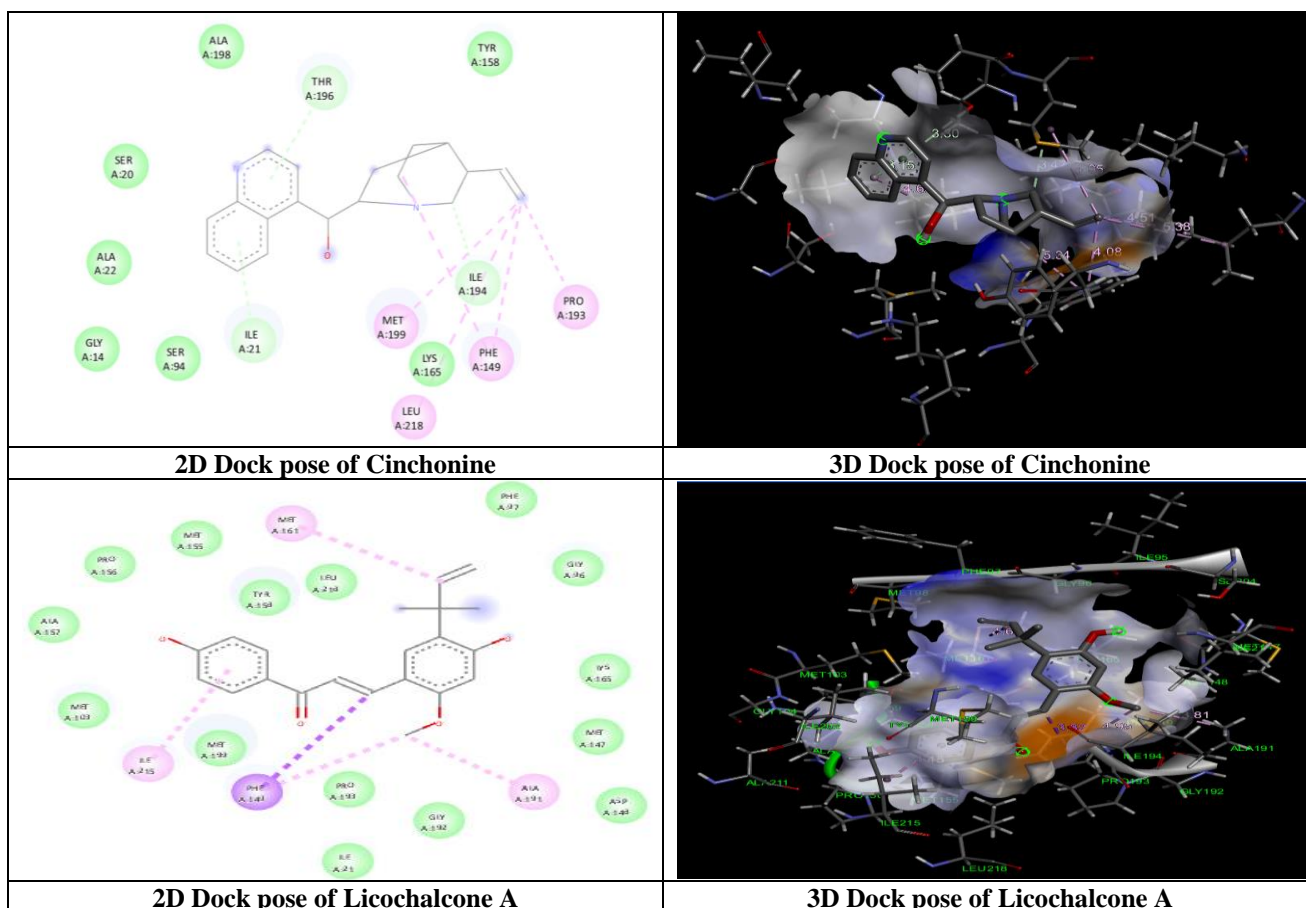


Fig 1. 2D and 3D dock poses of molecules.

### STRCURE ACTIVITY RELATIONSHIP

The structure–activity relationship (SAR) analysis was performed based on docking scores and molecular interaction patterns of the selected phytochemicals against the target protein (PDB ID: 4TZK). The observed binding affinities suggest that structural features such as aromatic ring systems, hydrogen bond donor/acceptor groups, and hydrophobic substituents play a critical role in stabilizing ligand–protein interactions within the active site.

Bilobetine exhibited the highest binding affinity (−10.4 kcal/mol), which may be attributed to its polycyclic aromatic framework combined with multiple oxygen-containing functional groups. The presence of hydroxyl and methoxy groups likely enhanced hydrogen bonding interactions with key residues such as LYS-165, MET-147, GLY-96, and MET-98. Additionally, its extended aromatic system facilitated  $\pi$ – $\pi$  stacking with PHE-148 and hydrophobic interactions with MET-199 and LEU-207, contributing to strong stabilization within the binding pocket. Compounds such as Tetrandrine and Lobenine (−8.9 kcal/mol) demonstrated that bulky alkaloid scaffolds with multiple ring systems favor hydrophobic and  $\pi$ -mediated interactions. Tetrandrine, with its bis-benzylisoquinoline structure, showed enhanced hydrophobic contacts, indicating that increased lipophilicity improves binding stability. Lobenine, on the other hand, displayed multiple hydrogen bond

interactions, suggesting that an optimal balance between hydrogen bonding capacity and aromatic character enhances activity. Flavonoid derivatives such as Sophoraflavanone G (−8.6 kcal/mol), Luteolin (−8.2 kcal/mol), Isoquiritigenine (−8.2 kcal/mol), and Licochalcone A (−7.8 kcal/mol) exhibited moderate to strong binding affinities. Their activity appears to correlate with the number and position of hydroxyl groups on the flavonoid backbone. The phenolic hydroxyl groups enhanced hydrogen bonding interactions, while the planar aromatic rings facilitated  $\pi$ – $\pi$  stacking with residues such as PHE-149. This suggests that planarity and electron-rich aromatic systems are favorable for interaction with the active site. Aloin and Cinchonine (−8.1 kcal/mol each) further highlight the importance of polar functional groups and rigid ring systems. Aloin, containing multiple hydroxyl groups and a glycosidic moiety, demonstrated strong hydrogen bonding capacity. Cinchonine, with its quinoline nucleus, promoted hydrophobic interactions and  $\pi$ -mediated stabilization within the binding pocket. In comparison, the reference drug Isoniazid (−5.2 kcal/mol), which possesses a relatively small and less complex structure, showed fewer hydrophobic and  $\pi$ -mediated interactions. This indicates that increased molecular complexity, aromatic surface area, and the presence of multiple hydrogen bond donors/acceptors significantly enhance binding affinity toward the target protein.

Overall, the SAR findings suggest that optimal inhibitory activity is associated with:

- (i) extended aromatic or polycyclic frameworks enabling  $\pi$ - $\pi$  interactions,
- (ii) appropriately positioned hydroxyl and methoxy groups facilitating hydrogen bonding, and
- (iii) hydrophobic substituents enhancing stabilization within the active pocket.

## CONCLUSION

The present molecular docking study demonstrated that the selected plant-derived compounds exhibited promising binding affinity against the target protein (PDB ID: 4TZK) when compared with the reference drug, Isoniazid. Among all tested molecules, Bilobetone showed the highest binding affinity, indicating strong interaction and stable complex formation within the active site. Several compounds, including Tetrandrine, Lobenine, Nolatrexed, and Sophoraflavanone G, also displayed significant binding potential supported by favorable hydrogen bonding and hydrophobic interactions. The interaction analysis highlighted the importance of key amino acid residues such as TYR-158, PHE-149, MET-199, and ILE-194 in ligand stabilization. Structure-activity relationship findings further suggested that aromatic frameworks, hydroxyl substitutions, and hydrophobic moieties play crucial roles in enhancing binding affinity. Overall, the results indicate that these phytocompounds may serve as potential lead molecules for further in vitro and in vivo validation studies aimed at developing novel therapeutic agents.

## ACKNOWLEDGMENT

The authors would like to express their sincere gratitude to Indubhai Patel College of Pharmacy & Research Center, Dharmaj for providing the necessary facilities and support for conducting this research. The guidance, infrastructure, and encouragement from the faculty and staff have been invaluable in completing this study.

## CONFLICT OF INTEREST

The authors declare that there is no conflict of interest.

## REFERENCES

1. Shah H, Patel J, Rai S, Sen A. Advancing tuberculosis elimination in India: A qualitative review of current strategies and areas for improvement in tuberculosis preventive treatment. *IJID Reg.*, 2025; 14: 100556.
2. Juliet A, Dave P, Marilyn M, Courtney L, Gillian T, David BA. Living with tuberculosis: a qualitative study of patients' experiences with disease and treatment. *BMC Public Health*, 2022; 22(1): 1717.
3. Salla AM, Simon AL, Helen JS, Mark EE, Atle F, Jimmy V. Patient adherence to tuberculosis treatment: a systematic review of qualitative research. *PLoS Med.*, 2007; 4(7): e238.
4. Lyon SM, Rossman MD. Pulmonary tuberculosis. *Microbiol Spectr*, 2017; 5(1).
5. Nardell EA. Extrapulmonary tuberculosis (TB). *MSD Manual Professional Edition*, 2022. <https://www.msdmanuals.com/professional/infectious-diseases/mycobacteria/extrapulmonary-tuberculosis/tb>
6. World Health Organization. Latent tuberculosis infection: updated and consolidated guidelines for programmatic management. Geneva: World Health Organization, 2018. <https://www.who.int/publications/i/item/9789241550239>
7. Centers for Disease Control and Prevention. Tuberculosis (TB). CDC, 2025. <https://www.cdc.gov/tb/>
8. Centers for Disease Control and Prevention. History of World TB Day. CDC. <https://www.cdc.gov/tb/worldtbd/history.html#9>
9. Daniel TM. The history of tuberculosis. *Respir Med.*, 2006; 100(11): 1862–1870.
10. Roberts CA, Buikstra JE. The bioarchaeology of tuberculosis: a global view on a re-emerging disease. Gainesville: University Press of Florida, 2003; 341.
11. Meachen GN. A short history of tuberculosis. London: John Bale, Sons & Danielsson Ltd., 1936.
12. Daniel TM, Bates JH, Downes KA. History of tuberculosis. In: Bloom BR, editor. *Tuberculosis: Pathogenesis, Protection, and Control*. Washington, DC: ASM Press, 1994; 13–35. doi:10.1128/9781555818357.
13. World Health Organization. Tuberculosis. Geneva: WHO; 2019. Available from: <https://www.who.int/news-room/factsheets/detail/tuberculosis>
14. World Health Organization. Global tuberculosis report 2023. Geneva: WHO; 2023. Available from: <https://www.who.int/teams/global-programme-on-tuberculosis-and-lung-health/tb-reports/global-tuberculosis-report-2023>
15. Chang CC, Crane M, Zhou J, Mina M, Post JJ, Cameron BA, et al. HIV and co-infections. *Immunol Rev.*, 2013; 254(1): 114–142. doi:10.1111/imr.12063.
16. Maison DP. Tuberculosis pathophysiology and anti-VEGF intervention. *J Clin Tuberc Other Mycobact Dis*, 2022; 27: 100300. doi:10.1016/j.jctube.2022.100300.
17. Nardell EA, Muzny CA. Tuberculosis (TB). In: *MSD Manual Professional Edition*. Kenilworth, NJ: Merck & Co., Inc.; 2022 <https://www.msdmanuals.com/professional/infectious-diseases/mycobacteria/tuberculosis-tb>
18. Tobin EH, Tristram D. Tuberculosis overview. In: *StatPearls [Internet]*. Treasure Island (FL): StatPearls Publishing; 2024 Dec <https://www.ncbi.nlm.nih.gov/books/NBK441916>
19. Trivedi A, Singh N, Bhat SA, Gupta P, Kumar A. Redox biology of tuberculosis pathogenesis. *Adv Microb Physiol*, 2012; 60: 263–324. doi:10.1016/B978-0-12-398264-3.00004-8.

20. Hoagland DT, Liu J, Lee RB, Lee RE. New agents for the treatment of drug-resistant Mycobacterium tuberculosis. *Adv Drug Deliv Rev.*, 2016; 102: 55–72. doi:10.1016/j.addr.2016.04.026.
21. Ahmad Z, Makaya NH, Grosset J. History of drug discovery: early evaluation studies and lessons learnt from them. In: Donald PR, van Helden PD, editors. *Antituberculosis chemotherapy. Prog Respir Res.* Basel: Karger, 2011; 3.
22. Dartois VA, Rubin EJ. Anti-tuberculosis treatment strategies and drug development: challenges and priorities. *Nat Rev Microbiol.*, 2022; 20(11): 685–701. doi:10.1038/s41579-022-00731-y.
23. Parikh SL, Xiao G, Tonge PJ. Inhibition of InhA, the enoyl reductase from Mycobacterium tuberculosis, by triclosan and isoniazid. *Biochemistry.*, 2000; 39(26): 7645–7650. doi:10.1021/bi0008940.
24. Rožman K, Sosič I, Fernandez R, Young RJ, Mendoza A, Gobec S, et al. A new “golden age” for the antitubercular target InhA. *Drug Discov Today.*, 2017; 22(3): 492–502. doi:10.1016/j.drudis.2016.09.009.
25. Ardiansah B. Chalcones bearing N, O, and S-heterocycles: recent notes on their biological significance. *J Appl Pharm Sci.*, 2019; 9(8): 117–129. doi:10.7324/JAPS.2019.90816.
26. Kaur H, Singh L, Chibale K, Singh K. Structure elaboration of isoniazid: synthesis, in silico molecular docking and antimycobacterial activity of isoniazid–pyrimidine conjugates. *Mol Divers.*, 2020; 24(4): 949–955. doi:10.1007/s11030-019-10004-1.
27. Chinnamulagund S, Joshi AS, Avunoori S, Kulkarni VH, Joshi SD, Joshi CD. Synthesis and antitubercular evaluation of certain pyrrole derivatives. *Indo Am J Pharm Res.*, 2023; 13(3). doi:10.5281/zenodo.7755252.
28. Deidda D, Lampis G, Fioravanti R, Biava M, Porretta GC, Zanetti S, et al. Bactericidal activities of the pyrrole derivative BM212 against multidrug-resistant and intramacrophagic Mycobacterium tuberculosis strains. *Antimicrob Agents Chemother.*, 1998; 42(11): 3035–3037. doi:10.1128/AAC.42.11.3035.
29. Patel S, Patadiya N. Preparation and standardization of Ayurvedic Nindra Vati. *Int J Pharm Sci.*, 2024; 2(2): 403–409. doi:10.5281/zenodo.10673390.
30. Dalvi D, Patel P, Dalvi H, Patel S, Patadiya N. Preparation and evaluation of herbal hair spray. *Int J Pharm Sci.*, 2024; 2(8): 3652–3659. doi:10.5281/zenodo.13367155.
31. Nikunj P, Shilpa P, Pooja M, Rikin P. Preparation and standardization of chitrakadi vati. *J Pharm Sci Innov.*, 2022; 11(3): 28–35. <http://dx.doi.org/10.7897/2277-4572.113230>.
32. Patel Y, Patel T, Patel S, Patel S, Patadiya N. Preparation and evaluation of herbal tooth powder using herbal resources. *Int J Pharmacogn Pharmaceut Sci.*, 2024; 6(2): 60–63. <https://dx.doi.org/10.33545/27067009.2024.v6.i2a.159>.
33. Patel R, Rathod D, Shah N, Vaghela V, Patadiya N. Inhibitors as a therapeutic frontier in lung cancer: Mechanism, opportunities, and molecular docking studies. *Comput Biol Med.*, 2025; 196: 110889. <https://doi.org/10.1016/j.compbiomed.2025.110889>.
34. Patadiya N, Teli A, Kazi S, Rathod P, Patel S. Preparation and evaluation of herbal mosquito repellent gel. *Int J Pharm Res Appl.*, 2025; 10(3): 1915–1921. doi:10.35629/4494-100319151921.
35. Joshi J, Vala B, Singh S, Patel S, Patadiya N. A review on natural molecules as pancreatic lipase inhibitor. *Res J Pharmacogn Phytochem.*, 2025; 17(2): 116–122. doi:10.52711/0975-4385.2025.00020.
36. Hire R, Richa D, Nikunj P. A validated, fast and simple, simultaneous determination of Captopril and Telmisartan in laboratory prepared mixture for use in haemodialysis patients suffering from inflammation. *Int J Pharm Qual Assur.*, 2023; 14(2): 255–261.
37. Nikunj P. Steroids: classification, nomenclature and stereochemistry. *Int J Univ Pharm Bio Sci.*, 2020; 9(5): 28–38.
38. Hetvi R, Misba V, Aman V, Shilpa P, Nikunj P. Preparation and standardization of Ayurvedic Triphala-Guggul Vati. *Int J Pharm Pharm Sci.*, 2025; 7(1): 135–139. <https://www.doi.org/10.33545/26647222.2025.v7.i1.b.162>.
39. Aman V, Hetvi R, Misba V, Shilpa P, Nikunj P. Method development for quantification of Gallic Acid in Triphala Guggulu Vati. *Int J Pharm Res Dev.*, 2025; 7(1): 312–318. <https://doi.org/10.33545/26646862.2025.v7.i1>.
40. Patadiya N, Vaghela V, Padhra S. Optimisation of synthetic condition for 2'-hydroxy chalcone by using mixture design. *Asian J Res Chem.*, 2023; 16(6): 417–422. doi:10.52711/0974-4150.2023.00068.
41. Patadiya N, Panchal N, Vaghela V. A review on enzyme inhibitors. *Int. res. j. pharm.*, 2021; 12(6): 60-6.
42. Patadiya N, Vaghela V. Design, in-silico ADME Study and molecular docking study of novel quinoline-4-on derivatives as Factor Xa Inhibitor as Potential anti-coagulating agents. *Asian Journal of Pharmaceutical Research*, Sep. 1, 2022; 12(3): 207-1. DOI: 10.52711/2231-5691.2022.00034
43. Dumpala RL, Patel J, Patadiya N, Patil C. Solubility and dissolution enhancement of Erlotinib by liquisolid compact technique. *International Journal of PharmaO2.*, 2020; 2(4): 0271-90.
44. Patadiya N, Dumpala R. A high profile review on new oral clotting factor Xa inhibitor: betrixaban. *Eur J Pharm Med Res.*, 2021; 8(1): 239-47.
45. Patel R, Darji J, Patadiya N, Thummar M. Development and evaluation of medicated chewing gum of raloxifene hydrochloride. *International Journal of Pharmaceutical and Biological Science Archive.*, 2021; 9(3): 01-12. <https://doi.org/10.32553/ijpba.v9i3.189>

46. Patadiya N, Vaghela V. An efficient method for synthesis of flavanone. *Asian Journal of Research in Chemistry*, May 1, 2022; 15(3): 221-4. DOI: 10.52711/0974-4150.2022.00039
47. Makvana P, Patadiya N, Baria D. Design, molecular docking, in-silico admet prediction, synthesis and evaluation of novel quinazoline derivatives as factor XA inhibitors. *Int. Res. J. Pharm.*, 2022; 13(3): 30-37. <http://dx.doi.org/10.7897/2230-8407.1303187>
48. Patadiya N, Vaghela V. An optimized method for synthesis of 2'hydroxy chalcone. *Asian Journal of Research in Chemistry*, 2022; 15(3): 210-2. DOI:10.52711/0974-4150.2022.00036
49. Tanuj Kolekar, Nikunj Patadiya, Self-emulsifying drug delivery Systems (SEDDS): A novel dissolution enhancement technique. *International Journal of Trend in Innovative Research*, 2020; 2(5): 10-20.
50. Soni D, Patadiya N. A wonderful hormone: estrogen. *International Journal of PharmaO2.*, 2020; 2(5): 0362-8.
51. Patadiya N, Vaghela V. A novel and eco-friendly method for Synthesis of 3-benzylidene-2-phenyl chroman-4-one analogs. *Asian Journal of Research in Chemistry*, May 1, 2022; 15(3): 195-9. DOI:10.52711/0974-4150.2022.00033
52. Kolekar T, Patadiya N. Dissolution enhancement technique: self-emulsifying drug delivery systems (SEDDS). *International Journal of Institutional Pharmacy and Life Sciences*, 2020; 10(6): 25-39.
53. Patel S, Patadiya N, Patel A. Formulation and Evaluation of Turmeric and Coriander Based Herbal Nail Polishes. *Int. J. of Pharm. Sci.*, 2024; 2(2): 488-95. <https://doi.org/10.5281/zenodo.10679282>
54. Patadiya N, Vaghela V. Design, Synthesis, Molecular Docking, In Silico ADMET, and Biological Evaluation of 3-Benzylidene-2-phenylchroman-4-one Derivatives as Pancreatic Lipase Inhibitors. *Russian Journal of Organic Chemistry*, 2025; 61(1): S155-66. DOI:<https://doi.org/10.1134/S107042802560247X>
55. Patadiya R, Shukla S, Patadiya N. Targeting InhA in Mycobacterium Tuberculosis: Recent Advances and Novel Scaffolds. *Asian Journal of Research in Chemistry*, 2026; 18(6): 378-384. DOI:10.52711/0974-4150.2025.00058